International Journal of Science and Research (IJSR)
ISSN (Online): 2319-7064
Index Copernicus Value (2013): 6.14 | Impact Factor (2013): 4.438

The Graphene Base DNA Sensing

Tarun M Radadiya

Student of Electronics & Communication Department of Vadodara Institute of Engineering, Gujarat Technological University (GTU), Vadodara, Gujarat, India

Abstract: ***Coupling nano materials with bio molecular recognition events represents a new direction in nanotechnology toward the development of novel molecular diagnostic tools. Here a graphene oxide (GO)-based multicolor fluorescent DNA nano probe that allows rapid, sensitive, and selective detection of DNA targets in homogeneous solution by exploiting interactions between GO and DNA molecules is reported. Because of the extraordinarily high quenching efficiency of GO, the fluorescent ssDNA probe exhibits minimal background fluorescence, while strong emission is observed when it forms a double helix with the specific targets, leading to a high signal-to-background ratio. Importantly, the large planar surface of GO allows simultaneous quenching of multiple DNA probes labeled with different dyes, leading to a multicolor sensor for the detection of multiple DNA targets in the same solution. It is also demonstrated that this GO-based sensing platform is suitable for the detection of a range of analytes when complemented with the use of functional DNA structures.***

Keywords: graphene oxide, DNA, biosensor, properties

1. Introduction

Graphene (or GO) is an excellent candidate for bio molecules anchoring and detection due to its large surface area (up to 2,630 m2/g) and unique sp2 (sp2/sp3)-bonded network. According to the binding affinity difference between single-stranded DNA (ss DNA) and double-stranded DNA (ds DNA) to graphene sheet, GO has been successfully adopted as a platform to discriminate DNA sequences. Fluorescent, electrochemical, electrical, surface-enhanced Raman scattering (SERS) and other methods have been utilized to achieve the sensitive, selective, and accurate DNA recognition.[1-10]

Recently graphene base biosensors have been use for detection of DNA molecules, The novel nonmaterial graphene with instructing electronics properties such as extraordinary strength, high thermal conductivity and main properties for biosensor biocompatibility, his significantly improve the sensors characteristics [11]. Graphene has been employed in biological system, such as detection Deoxyribonucleic acid (DNA), molecules and metal ions, proteins and pathogen, design of cell/bacterial neno devices and drug delivery carriers[12-15].graphene modified electrode would facilities electro transfer because it provides a non-cytotoxic ,large surface areas of immobilization[16,17].

DNA is biological macromolecules with double helix structure storing the hereditary information of life. understanding the information encode in DNA is essentially for biomedical and medical research , DNA sequence consist of the series of a symbol representing the nucleotide base : adenine(A), thymine (T),guanine (G) ,and cytosine (C),with can interact with graphene.

2. DNA Sequencing with Graphene Nanopores

The aim of DNA sequencing is to obtain the order of DNA composition comprising the base pairs A (adenine) T (thymine), and C (cytosine) G (guanine). The fast development of DNA sequencing technology allows us to better understand the relationships among diseases, inheritance, and individuality. Solid state nanopores have been recommended as the next generation platform for DNA sequencing due to its low-cost and high-throughput.

DNA translocation through single-layer graphene nanopores of different diameters under conditions of various ion concentrations and applied voltages; DNA translocation through multilayer graphene nanopores varied from a single to a few layers; pulling out single strand DNA molecules from small graphene nanopores of different geometries. The thickness of graphene sheet (~0.344nm) is in the range of the nucleotide distance in single strand DNA (ssDNA) (0.32-0.52nm). This means that a graphene nanopore can only interact with one nucleotide at the same time. This special property of the graphene nanopore makes it a star material for DNA sequencing [18].

Graphene nanopores have been investigated in DNA sequencing due to their single-atom thickness and unique mechanic properties. They have been used widely in DNA detection in recent years[19-21]. In this work, single molecule sequencing with graphene nanopores to identify four bases was investigated by molecular dynamics (MD) simulation. Table 1 lists all the MD simulations we performed in various conditions. As shown in Figure.1, an ssDNA molecule was observed translocating through a graphene nanopore under a certain electric field and the translocation time was calculated to distinguish different types of bases. In this figure, the starting time *t1* is defined as the time when the first atom of the DNA molecule starts to enter into the nanopore and the end time *t2* is defined as the time when the DNA molecule exit the nanopore completely. The time interval between *t1* and *t2* is defined as the DNA translocation time. By characterizing the profile of the translocation time for the DNA passing through graphene nanopores of different diameters under various applied electric fields, we are able to distinguish the nucleotides of the DNA.

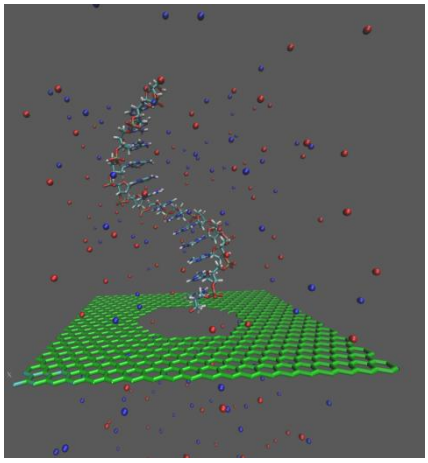

Figure 1: Initial structure of a system with an ssDNA and a graphene nanopore. K+ ions are in blue and Cl^- ions in red. The water molecules are not shown for clarity.

To construct a graphene nanopore, the graphene sheet was set in the *x*-*y* plane with its center of mass in the origin (0, 0, 0) of the Cartesian coordinate, and the atoms with their coordinates satisfying $x^2 + y^2 < r^2$ were deleted, where *r* is the radius of the graphene nanopore. ssDNA fragments with different nucleotide compositions (as shown in Table 1) were constructed by using the Hyperchem software (Version 8.0, Hypercube, Inc). Each system, which consists of a nanopore and an ssDNA fragment, was solvated in a box of TIP3P[22] water molecules and underwent a 50000-step energy minimization. 14 K+ were added into the system as counterions. Then, KCl ions were added into the box to match the same concentration as used in experiment[23].

The DNA and KCl were modeled by the CHARMM27 force field[24] and all the carbon atoms in the graphene sheet were set to be neutral. The force field parameters for graphene were obtained from our previous work, with σCC = 0.385 nm and εCC = -0.439 kcal/mol.[25,26] All simulations were performed by the GROMACS 4.5.2 program[27].The periodic boundary condition was applied to model the infinite graphene nanopore and the particle mesh Ewald summation was used to recover the long range electrostatic interaction, with a cutoff of 1.3 nm for the separation of the direct and reciprocal space summations. All atoms including hydrogen atoms were represented explicitly and the lengths of the bonds containing hydrogen atoms were fixed. The cutoff for the non-bonded van der Waals interaction was set by a switching function starting at 1.0 nm and reaching zero at 1.2 nm. The time step is 2 fs. The Langevin method was employed to keep the temperature at 298 K with the pressure set at 101.3 kPa. Different bias voltages were applied in the simulations to drive the ions and ssDNA passing through the nanopores.

3. Effect of Graphene Diameter on DNA Translocation

With the graphene nanopore of 1.6nm in diameter, the translocation time for the nucleotides is rather long. Of poly(A)15, poly(T)15, poly(C)15 and poly(G)15, none was observed to translocate through the nanopore completely in our simulations carried out for 50 ns under the electric field from 100mv/nm to 600mv/nm (SimIA1-SimIG4 in Table 1).

	Number of atoms	Electric field (mv/nm)	Diameter of the pore (nm)	KCl Concentration (M)	DNA (bp)	Time (ns)
SimIA1	41,564	100	1.6	1.0	poly(A)15	50
SimIT1	41,246	100	1.6	1.0	poly(T)15	50
SimIC1	41,504	100	1.6	1.0	poly(C)15	50
SimIG1	41,335	100	1.6	1.0	poly(G)15	50
SimIA2	41,564	200	1.6	1.0	poly(A)15	50
SimIT2	41,246	200	1.6	1.0	poly(T)15	50
SimIC2	41,504	200	1.6	1.0	poly(C)15	50
SimIG2	41,335	200	1.6	1.0	poly(G)15	50
SimIA3	41,564	400	1.6	1.0	poly(A)15	50
SimIT3	41,246	400	1.6	1.0	poly(T)15	50
SimIC3	41,504	400	1.6	1.0	poly(C)15	50
SimIG3	41,335	400	1.6	1.0	poly(G)15	50
SimIA4	41,564	600	1.6	1.0	poly(A)15	50
SimIT4	41,246	600	1.6	1.0	poly(T)15	50
SimIC4	41,504	600	1.6	1.0	poly(C)15	50
SimIG4	41,335	600	1.6	1.0	poly(G)15	50
SimIA5	41,735	100	2.0	1.0	poly(A)15	30
SimIT5	42,705	100	2.0	1.0	poly(T)15	30
SimIC5	42,713	100	2.0	1.0	poly(C)15	30
SimIG5	41,938	100	2.0	1.0	poly(G)15	30
SimIA6	41,735	200	2.0	1.0	poly(A)15	10
SimIT6	42,705	200	2.0	1.0	poly(T)15	10
SimIC6	42,713	200	2.0	1.0	poly(C)15	10
SimIG6	41,938	200	2.0	1.0	poly(G)15	10
SimIA7	41,735	400	2.0	1.0	poly(A)15	10
SimIT7	42,705	400	2.0	1.0	poly(T)15	10
SimIC7	42,713	400	2.0	1.0	poly(C)15	10
SimIG7	41,938	400	2.0	1.0	poly(G)15	10
SimIA8	41,735	600	2.0	1.0	poly(A)15	10
SimIT8	42,705	600	2.0	1.0	poly(T)15	10
SimIC8	42,713	600	2.0	1.0	poly(C)15	10
SimIG8	41,938	600	2.0	1.0	poly(G)15	10
SimIA9	41,735	50	2.0	1.0	poly(A)15	50
SimIT9	42,705	50	2.0	1.0	poly(T)15	50
SimIC9	42,713	50	2.0	1.0	poly(C)15	50
SimIG9	41,938	50	2.0	1.0	poly(G)15	30
SimA5	42,831	100	2.0	0.0	poly(A)15	30
SimT5	43,961	100	2.0	0.0	poly(T)15	30
SimC5	43,921	100	2.0	0.0	poly(C)15	30
SimG5	43,105	100	2.0	0.0	poly(G)15	30

The reason is that the diameter of ssDNA (~ 1.1nm) is almost comparable to that of the nanopore(1.6nm), which makes it difficult for the DNA to pass through completely in the limited simulation time due to the steric effect. Based on our previous work, [28] a large graphene nanopore can facilitate the translocation of ssDNA but decrease the identification at single nucleotide resolution. To achieve a balance between simulation time and resolution, a 2.0nm graphene nanopore was selected for sequencing the DNA in our simulations. We found that poly(A)15, poly(T)15, poly(C)15, and poly(G)15 can translocate through the

nanopore under the electric field of 100mv/nm (SimIA5-SimIG5 in Table 1) within 30 ns. The averaged blockade currents during the translocation of different nucleotides were calculated from the simulations (SimIA5-SimIG5 in Table 1),as shown in Figure 2.

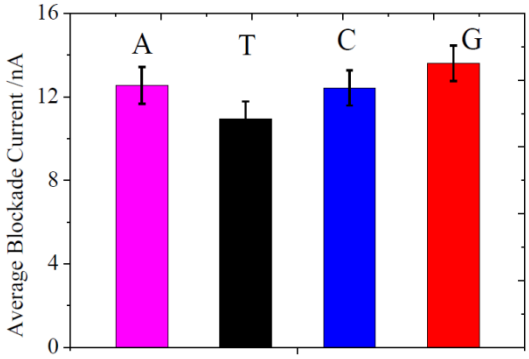

Figure 2: The averaged blockade currents of different nucleotides poly(A)15, poly(T)15, poly(C)15, and poly(G)15 in the 2 nm graphene nanopore under the electric field of 100mv/nm.

One can see that the order of the averaged blockade currents is T < C < A < G. Compared with the experimental order T < G< C<A, the order of T, C, A is in accordance with the experiment one [29], with the exception that the blockade of G is much smaller than A in the experiment; however, the error rate in the experiment is always with the high blockade current of G which means the blockade current for G is not so stable. The results show us our simulation could be used to descirbe the process of DNA than slocation. The reason of blockade of G is much bigger than that in experiment is that the applied electric field (100mv/nm) in these simulations is much larger than that in experiments, which makes it difficult to distinguish the blockade currents between A and G. Our results show that T and G can be identified from the blockade current very clearly since the blockade current for T is much smaller than that for G, which has been also observed experimentally[28,31]. However, the difference in the blockade current between A and C is too small to be distinguishable with the 2 nm graphene nanopore. Another interesting phenomenon is that all the nucleotides tend to adsorb on the graphene nanopore surface after translocation. This observation has also been confirmed by the experimental and theoretical works [21, 30].

4. Graphene Nanoprobe DNA Analysis

Graphene is an one-atomthick 2D nano material with extraordinary electronic, thermal, and mechanical properties,[32,33] which, along with its water-soluble derivative, graphene oxide (GO),has become extremely popular in nanoelectronics and nanocomposites.[34–36] However, biological applications of graphene and GO remain to be explored.[37,38] Of our particular interest, graphene was recently predicted through theoretical calculations to be a superquencher with the long-range nanoscale energy transfer property,[39,40] which, in combination with the unique DNA/GO interactions, forms the basis of a convenient and versatile strategy for multicolor fluorescent DNA analysis. Very recently, and during the preparation process of the current work, Lu et al. reported that GO could bind and quench a dye-labeled single-stranded DNA (ssDNA) probe; the fluorescence was recovered when the probe formed a duplex with its target, which released the probe from GO.[40] We herein report a new graphene-based strategy that allows multicolor DNA analysis in the same solution and a mix-and-detect assay format with significantly improved sensitivity and speed show in figure 3.

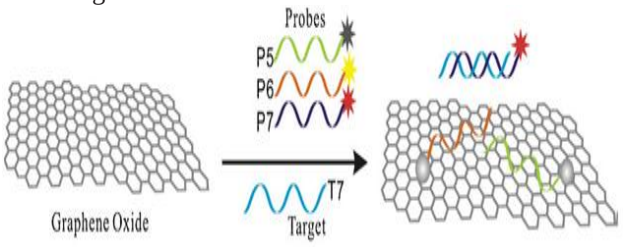

Figure 3: for the GO-based multicolor DNA analysis. Fluorescence spectra of mixture probes (P5, P6, and P7) in the presence of different targets T5 (blue), T6 (red) and T7 (orange) with the excitation wavelengths of 494, 643, and 587 nm.

Table 2: DNA sequences

Oligonucleotide	Sequence
P1: FAM-tagged probe	5′ -FAM- TCGTTGGAGTTTGTCTG-3′
T1: target for P1	5′-CAGACAAACTCCAACGA-3′
R1: random sequence	5′-GCAGAGCCAGTTCCAAG-3′
M1: single-base mismatched target for P1	5′-CAGACA AATTCCAACGA-3′
M2: single-base mismatched target for P1	5′-CAGACA AAATCCAACGA-3′
M3: single-base mismatched target for P1	5′-CAGACA AAGTCCAACGA-3′
T2: long target for P1 (complementary part in the middle)	5′-ATTTCACTGACAGTTCAGACAAACTCCAAC GACTAGCTACGTGCCGA-3′
T3: long target for P1 (complementary part at the 5′-end)	5′ -CAGACAAACTCCAACGACTAGCTATG TGCCGAATTTCAAGGACAGTT-3′
T4: long target for P1 (complementary part at the 3-end)	5′-CTAGCTATGTGCCGAATTTCAA GGACAGTTCAG ACAAACTCCAACGA-3′
P5: FAM-tagged P16 probe	5′ -FAM-CAGAGGCAGTAACCA-3′
T5: target for P5	5′-TGGTTACTGCCTCTG-3′
P6: Cy5-tagged P21 probe	5′ -Cy5-CCCTAATCCGCCCAC-3′
T6: target for P6	5′-GTGGGCGGATTAGGG-3′
P7: ROX-tagged P53 probe	5′ -ROX-CCTGGTGCCGTAGAT-3′
T7: target for P7	5′-ATCTACGGCACCAGG-3′

P8: MSO probe for Hg^2	5′ -FAM-TTCTTTCTTCCCCTTGTTTGT T-3′
P9: Adenosine probe (Underlined part is the anti-adenosine aptamer sequence)	5′ -FAM-TAATTACCTGGGGGAGTATTGCGGAG GAAGGTTAT -3′

P5: 5′-FAM- CAGAGGCAGTAACCA-3′
P6:5′-Cy5-CCCTAATCCGCCCAC-3′
P7:5′-ROX-CCTGGTGCCGTAGAT-3′
T7:5′-ATCTACGGCACCAGG-3′

Analysis of DNA sequencing by reducing graphene oxide

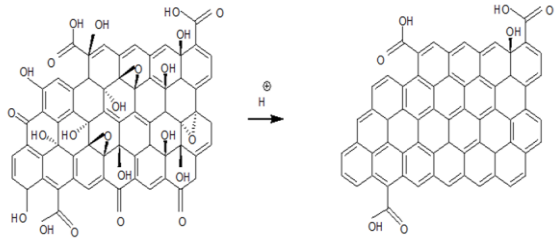

The H ion reduces the graphene oxide. The addition of H ion shifts the pH to acidic side. The graphene oxide is soluble at high pH and aggregates are formed at low pH. This property of graphene oxide is applied in the measurement of released H ion by measuring shift in pH signal during DNA polymer synthesis [41-47]. The flow of nucleotides base is controlled in the sequence of A, G, C and T. The addition of nucleotide is sensed by shift in pH, non-addition make a blank shift and repetitive addition by proportional shift. The Equations of reading of adding nucleotide to the complimentary template strand by capture of H ion resulting in shift of pH on reduction of graphene oxide sensor is:

T + A = T...A + H_+ ΔpH Eq. (1)
T...A+A = T...A+A
T...A+G = T...A+G
T...A+C = T...A+C
T...A+T = T...A…T + H_+ ΔpH Eq. (2)

T...A…T+A = T...A…T+A
T...A…T+G = T...A…T…G + H_+
ΔpH Eq. (3)

The equations 1-3 described the sequencing of 3 nucleotide base units in addition to initial nucleotide with the release of H ion captured by shift in pH by reducing graphene oxide. The cycle moves on the addition of nucleotide base on the complimentary template strand. The template strand of upto 200 nucleotides is sequenced by this method. The template strand is enzymatically fragmented from the genomic DNA for error free short strand sequencing. The pH shift of 4 to 1 corresponds to synthesis cycle of 3 nucleotide bases from the initial base. The shift in pH cycle goes on to read the nucleotide base addition in the synthesis cycle. The pH shift by reduction of graphene oxide with released H ion during polymer synthesis.

5. DNA Biosensing Employing Graphene Platform

Although the nucleobases graphene binding energy is slightly different via various strategies and equipments, one might be certain that ssDNA could be adsorbed on graphene sheet surface coupling crossover of several interaction forces and employing nucleobases as the anchors. This is also the root cause that ssDNA binds more strongly to graphene than dsDNA does [48], in which nucleobases are entrapped and shielded by the phosphate deoxyribose backbones. According to the binding affinity difference between ssDNA and dsDNA to graphene sheet, graphene (GO) has been successfully adopted as a platform to discriminate DNA sequences. Several methods, such as fluorescent, electrochemical, electrical, and SERS, have been utilized to achieve the sensitive, selective, and accurate DNA recognition.

In a typical fluorescent manner (Figure:4a) [49], fluorescent dye-labeled ssDNA was adsorbed on graphene surface. Then, the fluorescence of dye-labeled ssDNA was completely quenched due to the fluorescent resonance energy transfer (FRET). In the presence of a target, the hybridization between dye-labeled ssDNA and target sequence altered the conformation of ssDNA and disturbed the binding between the dye-labeled ssDNA and graphene. This behavior might originate from the fact that DNA nucleobases matching is more energetically favorable than binding with graphene. The formed dye-labeled dsDNA left from graphene surface, resulting in the restoration of dye fluorescence. Based on the mechanism, both hairpin DNA and molecular beacon (MB) were designed for homogeneous DNA detection [50, 51].

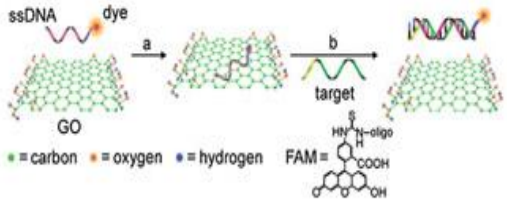

(a)

Figure 4: (a) Schematic representation of the target-induced fluorescence change of the ssDNA–FAM–GO complex. FAM is the fluoresce in-based fluorescent dye.

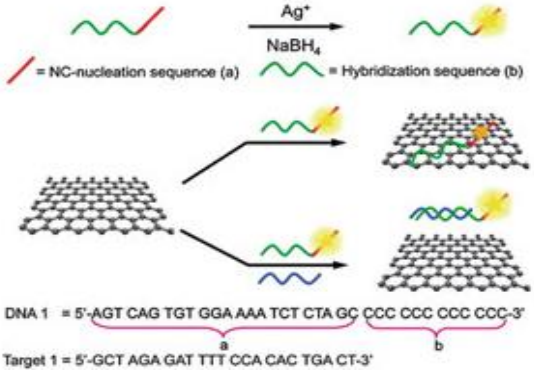

Figure 4: (b) Schematic representation of the preparation of silver nanoclusters on DNA scaffolds in aqueous solution and the assay for DNA detection using AgNCs-GO nanohybrid materials.

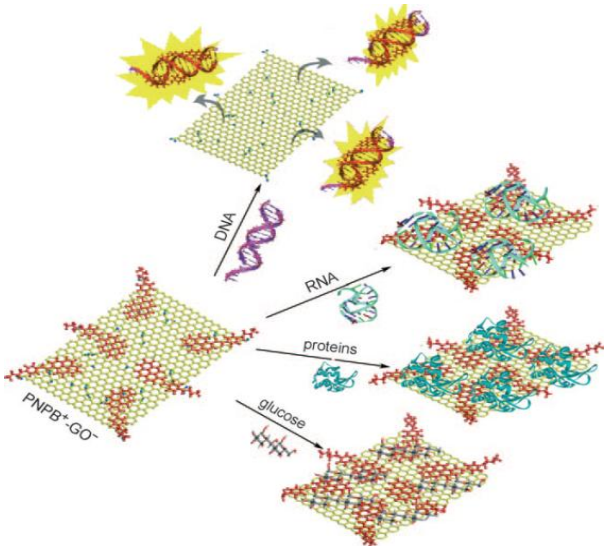

Figure 4: (c) Sensing by PNP+GO−. DNA can complex efficiently with PNP+ to form ionic complex PNP+DNA− and thus switches on the fluorescence. Other biomolecules undergo π–π stacking on GO but do not remove PNP+ from GO, and thus, fluorescence remains quenched

dsDNA was also detected by the formation of triplex DNA with dye-labeled ssDNA [53]. As a nanoquencher, graphene shows super-quenching capacity with a wide energy transfer range, which may quench the fluorescence of different dyes simultaneously. Fan and coworkers devised a multicolor fluorescent DNA analysis manner [52], in which multiple ssDNA sequences labeled with different dyes were anchored on graphene. Hybridization to multiple DNA targets in the same solution led to fluorescence recovery of different dyes. The multicolor biosensor might also be suitable for the detection of a range of analytes. Due to the different graphene fabrication methods, the carbon-to-oxygen (C/O) ratios in GO might differ at a large level, also the sp3/sp2 bonded network structure. This may have a great impact on GO's ability for fluorescence quenching of adsorbed dyes and the binding interactions to ssDNA, resulting in a broad range of DNA detection sensitivity. In fact, rGO, in which the oxygenic groups are partially or totally reduced, might not be directly used in the detection due to the strong tendency to aggregate [54]. To get a deeper insight into this, properties of GO samples with tuned C/O ratios (1.1, 1.3, 1.6, and 1.9) were fairly investigated [55]. Results showed that GO with high C/O ratio bound more strongly to ssDNA and quenched the fluorescence of organic chromophores more effectively than that with low C/O ratio. The loading amount of fluorophore-labeled ssDNA at least oxidized GO (C/O ratio = 1.9) was four times than that at GO with C/O ratio of 1.1. With the tunable chemical compositions, GO nanosheets offer a broad range of materials with different fluorescence quenching efficiencies and binding affinity with ssDNAs, which exhibit the great potential in biological applications.

6. Metallic Graphene Nano ribbon with a Nanopore

However, the tunneling-current based graphene biosensors will face the same challenges[69]encountered by current experimental efforts to utilize transverse tunneling current across a gap between two gold electrodes, [60,61] such as poor Signal-to-noise ratio at small bias voltages due to the fact that molecular eigenlevels are typically far away from the Fermi energy of the electrodes. In this case, the tunneling is offresonant and currents are of the order of picopampere at typically applied[60,61] bias voltage 0.5 V. Such small off-resonant tunneling currents are highly dependent on difficult-to-control relative geometry between the molecule and electrodes, so that recent experiments have measured broad current distributions corresponding to each nucleotide in the case of bare gold electrodes[60] and somewhat narrower but still overlapping distributions18 for functionalized gold electrode

Its operation crucially relies on the existence of metallic nanowires in which the spatial current profile[62] is confined around their transverse edges, so that drilling a nanopore in their interior should not change significantly their conductance which is of the order of few conductance quanta 2e2/h.

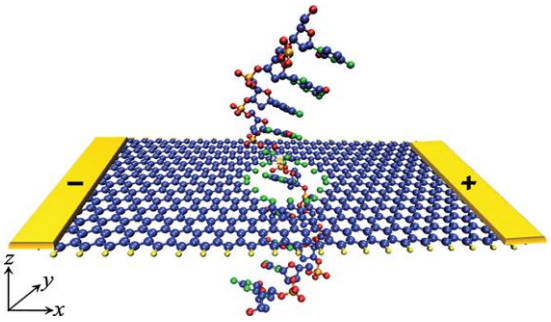

Figure 5. Schematic view of the proposed two-terminal device where transverse conduction current flows mostly around the zigzag edges of a metallic graphene nanoribbon with a nanopore, while DNA molecule is translocated through the pore to induce nucleobase-specificmodulation of such edge currents. The active device region, which is simulated via first-principles quantum transport formalism, consists of a segment of 14-ZGNR (composed of 14-zigzag chains that determine its width ~3.1 nm) and a nanopore of ~1.2 nm diameter. The edge carbon atoms of the nanopore are passivated by either hydrogen or nitrogen, while edge atoms of ZGNR itself are passivated by hydrogen. The total number of simulated atoms (C-blue, H-yellow, N-green, Ored, P-orange) in the active region, including the nucleobase within the nanopore, is around 700.

When one of the four nucleobases of DNA, adenine (A), cytosine (C), guanine (G), or thiamine (T), is inserted into the nanopore in the course of DNA translocation, it will affect the charge density around the pore thereby modulating edge conduction currents that are several orders of magnitude larger than tunneling currents across nanogaps[56,70,57,58,60,61] or nanopores in AGNRs[59] (where edge currents are absent). The large operating current may also remove the need to slow down or constrain the DNA molecule as it translocates, since the measurement speed may be high enough to prevent Brownian fluctuations of the molecule from blurring the signal. The candidate nanowires supporting edge currents can be found among GNRs with zigzag edges or the very recently fabricated [63] chiral GNRs, as well as among two-dimensional topological insulators (2D TI).[64] In the case of zigzag or chiral GNRs,

spatial profile of local currents carried by electrons around the charge neutral point (CNP) shows large magnitude around the edge[65] and a tiny current flowing through their interior. In 2D TI nanowires, similar situation will appear if the wire is narrow enough so that helical edge states overlap slightly and edge currents can be modulated. Otherwise, in sufficiently wide 2D TI wires current is strictly confined to the edges and cannot be affected by time-reversal-preserving impurities, vacancies, or modulation of charge density because of the fact that helical edge states guide electrons of opposite spin in opposite directions to prevent their backscattering.[64] We note that recent first-principles analysis has suggested that GNRs could also be converted into 2D TI wires via heavy adatom deposition in order to increase the spin−orbit coupling.[66] The recent proliferation of nanofabrication techniques[63,67,68] for GNRs with ultra smooth edges is making them widely available, and their exposed surface allows for an easier integration into biosensors. Therefore, in the device depicted in Figure 5 we choose to consider a GNR with zigzag edges (ZGNR). Note that edge currents in ZGNRs have already been confirmed in experiments where they were exploited to increase heat dissipation around edge defects and, thereby, rearrange atomic structure locally until sharply defined zigzag edge is achieved [68]

7. Field-effect graphene for all-electrical DNA

create an 8-FET DNA sensor array fabricated from CVD graphene, with two key features representing steps towards multiplexed graphene DNA arrays. First, 7 out of the 8 FETs achieve a maximum sensitivity of 100 fM, demonstrating a robust array yield with the sub-picomolar sensitivity. This sensitivity is 10 times higher than the prior state-of-the-art CVD graphene FET DNA sensor [75] and is on par with if not better the ~1pM sensitivity of industry-standard optical DNA microarrays[73,74,77] which finds a range of molecular diagnostic applications in research and clinical settings. While certain high-end optical and electrochemical DNA sensors[78-85] achieve a far higher sensitivity down to the sub-fM level, our device is more advantageous in achieving chip-scale integration and label-free operation simulataneously[71,72,75]. Second, each graphene site in the array is used not only as a sensing FET but also as an electrophoretic electrode to enable site-specific immobilization of probe DNA. Specifically, when probe DNA of a particular sequence desired at specific graphene sites is introduced into the electrolyte overlying the device array, these graphene sites are positively biased to attract and anchor the probe DNA molecules, while the rest of the graphene sites are negatively biased to repel them. This use of graphene as an electrophoretic electrode for DNA immobilization is an adaptation of electrophoretic DNA immobilization using conducting electrodes of different materials (for example, Pt, Au and carbon paste) [86-89]. The resulting site-specific single-stranded probe DNA array then enables site-specific detection of singlestranded target DNA upon hybridization, where this detection phase uses each graphene as a FET. That is, graphene engaged in the dual role of electrophoretic electrode and sensing FET enables site-specific operation of graphene DNA array in an all-electrical manner (in both probe assembly and target detection), offering possibilities for highly multiplexed graphene DNA arrays.

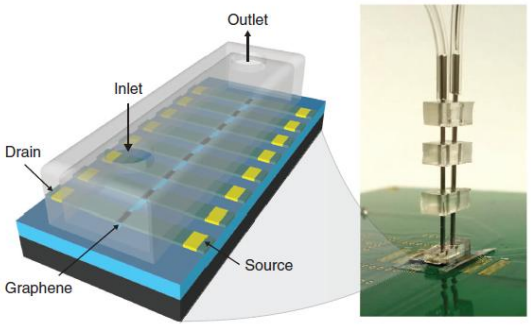

Figure 6: (a) Illustration and image of an 8-graphene-electrode/FET array with a microfluidic channel on top. This entire device sits on a printed circuit board.

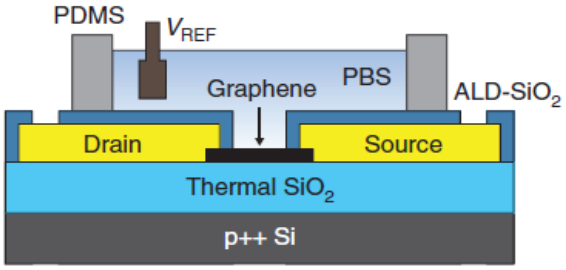

Figure 6: (b) Cross-sectional illustration of an individual graphene site.

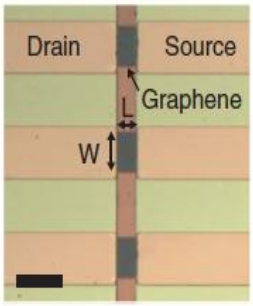

Figure 6: (c) Optical micrograph of a portion of a fabricated graphene array. For an individual graphene site, W=90 μm and L=45 μm (scale bar, 120 μm).

The array fabrication starts by transferring CVD-grown, monolayer-dominated graphene onto a SiO2/Si substrate [91, 92]. We pattern this graphene sheet into a linear array of eight local graphene sites by oxygen-plasma etching, with a graphene-to-graphene pitch of 240 μm. Contacts are made to both ends 'source' and 'drain' of each graphene site with Cr/ Au/Cr metals, with the remaining graphene channel being 45-μm long and 90-μm wide (Figure. 1). To obviate the leakage current from these metal contacts to the electrolyte [93, 94] we passivate the metal contacts by depositing a SiO2 layer. A polydimethylsiloxane microfluidic channel is fabricated on top of the array to facilitate robust, controllable delivery and clearing of DNA molecules as well as materials to functionalize graphene surface. An Ag/AgCl wire immersed in the electrolyte inserted into the outlet tube serves as a reference electrode. Before the site-specific operation of the array with each graphene site acting as an electrophoretic electrode as well as a sensing FET, we first passively immobilize probe DNA molecules of the same sequence all across the array without site specificity that is, here graphene is not used as an electrode for site-specific

immobilization and measure the sensitivity limit of each graphene FET.

8. Graphene-based fret biosensors

Table 3: FRET biosensors fabricated with graphene-based nanomaterials

Graphene category	Probe type	Probe sequence	Target	LO(nM)	Refs
Graphene	ssDNA	5′-FAM-AATCAACTG GGA GAATGTAACTG-3′	cDNA	N/A	[94]
Graphene oxide	ssDNA	5′-FAM-AGTCAGTGTGGAAAATCTCTAGC-3′	cDNA	N/A	[96]
Graphene oxide	Aptamer	5′-FAMTCTCTCAGTCCGTGGTAGGGCAGGTTGGGG TGACT-3′	Human thrombin	2.0	[96]
Graphene oxide	ssDNA and dsDNA	5′-FAMGGAATTCTAATGTAGTATAGTAATCCGCTC-3′ 5′-(T)15GAGCGGATTACTATACTACATTAGAATTCC-3′	SCV helicase	0.625	[97]
Graphene oxide	ssDNA	5′-FAM- TCGTTGGAGTTTGTCTG-3′ 5′-Cy5-CCCTAATCCGCCCAC-3′ 5′-ROX-CCTGGTGCCGTAGAT-3′	cDNA	0.1	[98]
Graphene oxide	Hairpinstructured DNA	5′-Dabcyl- CGACGGAGAAAGGGCTGCCACGTCG -FAM-3′	cDNA	0.2	[99]
Graphene oxide	Aptamer	5′-FAMCTCTCTTCTCTTCATTTTTCAACACAACACA C-3′	Silver (I) ions	5	[100]
SDBS graphene	Aptamer	5′-FAM-GGTTGGTGTGGTTGG-3′	Bovine thrombin	0.0313	[101]
Graphene oxide	MB	5′-Dabcyl-CGACGGAGAAAGGGCTGCCACGTCG-Cy5-3′	survivin mRNA	N/A	[102]
Graphene oxide	ssDNA	5′-H2N-(T)6GCACACGCGCAC-3′	Au NPlabeled cDNA	200	[103]

There is increasing interest in the use of graphene for the development of FRET biosensors. FRET involves the transfer of energy from a donor fluorophore to an acceptor fluorophore, and is one of the advanced tools available for measuring nanometer-scale distance and changes, both in vivo and in vitro [104]. Recent theoretical and experimental studies have shown that graphene can be a highly efficient quencher for various organic dyes and quantum dots (QDs) [105]. Compared with organic quenchers, graphene has shown superior quenching efficiency for a variety of fluorophores, with low background and high signal-to-noise ratio [94,95]. Graphene and GO have been reported to interact strongly with nucleic acids (NAs) through p–p stacking interactions between the ring structures in the NA bases and the hexagonal cells of graphene and GO; whereas double-stranded DNA (dsDNA) cannot be stably adsorbed onto the surface because of efficient shielding of nucleobases within the negatively charged dsDNA phosphate backbone [96,97]. The development of graphene based FRET biosensors has been motivated greatly by reliance on this particular principle and integrating it with the advantages of graphene. Here, we selectively summarize recent progress in biosensors that integrate the super quenching property of graphene and the recognition properties of NAs (Table 3).

The first graphene-based FRET biosensor included a fluorescein amidite (FAM)-labeled ssDNA adsorbed onto GO [96]. As a result of the FRET effect between FAM and GO, fluorescence is quenched rapidly however, binding between probe ssDNA and a complementary ssDNA alters the conformation, and consequently, releases FAM ssDNA from the GO surface and results in fluorescence recovery. Detection of cDNA is therefore realized. Similarly, multicolor DNA analysis has been accomplished with graphene based FRET biosensors [98]. The planar GO surface allows simultaneous quenching of multiple ssDNA probes labeled with different dyes, which leads to a multicolor sensor for the detection of multiple DNA targets. In this case, a graphene-based FRET biosensor is able to detect different DNA targets with various sequences by using ssDNA probes with different sequences. In another example, a graphene-based FRET platform has been developed for detection of helicase-mediated unwinding of duplex DNA [97]. By reliance on the preferential binding of GO to ssDNA over dsDNA, the dsDNA substrate that contains a fluorescent dye at the end of one strand is prepared first. As helicase unwinding of dsDNA proceeds, the fluorescence decreases and is quenched completely because of strong interaction of GO with unwound ssDNA. Helicase activity can thus be monitored in real time.

9. Conclusion

Graphene is excellent material for the DNA sequence sensing and interact with graphene nanopore and graphene Nanoprobe. No of new and more different sensing method and more no of DNA sequence using graphene. graphene made DNA sensor low cost, , more efficiency ,very sensitive, more flexible .

References

[1] He, S., Song, B., Li, D., Zhu, C., Qi, W., Wen, Y., Wang, L., Song, S., Fang, H., Fan, C.: A graphene nanoprobe for rapid, sensitive, and multicolor fluorescent DNA analysis. Adv. Funct. Mater. 20, 453–459 (2010)

[2] Liu, F., Choi, J.Y., Seo, T.S.: Graphene oxide arrays for detecting specific DNA hybridization by fluorescence resonance energy transfer. Biosens. Bioelectron. 25, 2361–2365 (2010)

[3] Bonanni, A., Pumera, M.: Graphene Platform for Hairpin-DNA-Based Impedimetric Genosensing. ACS Nano 5, 2356–2361 (2011)

[4] Lu, C.H., Yang, H.H., Zhu, C.L., Chen, X., Chen, G.N.: A graphene platform for sensing biomolecules. Angew. Chem. Int. Ed. 48, 4785–4787 (2009)

[5] Li, F., Huang, Y., Yang, Q., Zhong, Z., Li, D., Wang, L., Song, S., Fan, C.: A graphe neenhanced molecular beacon for homogeneous DNA detection. Nanoscale 2, 1021–1026, (2010)

[6] Lu, C.H., Li, J., Liu, J.J., Yang, H.H., Chen, X., Chen, G.N.: Increasing the sensitivity and single-base mismatch selectivity of the molecular beacon using graphene oxide as the "nanoquencher". Chem.-Eur. J. 16, 4889–4894 (2010)

[7] Hu, Y., Li, F., Bai, X., Li, D., Hua, S., Wang, K., Niu, L.: Label-free electrochemical impedance sensing of DNA hybridization based on functionalized graphene sheets. Chem. Commun. 47, 1743–1745 (2011)

[8] Dubuisson, E., Yang, Z., Loh, K.P.: Optimizing label-free DNA electrical detection on graphene platform. Anal. Chem. 83, 2452–2460 (2011)

[9] Hu, Y., Li, F., Han, D., Wu, T., Zhang, Q., Niu, L., Bao, Y.: Simple and label-free electrochemical assay for signal-on DNA hybridization directly at undecorated graphene oxide. Anal. Chim. Acta 753, 82–89 (2012)

[10] Tang, Z., Wu, H., Cort, J.R., Buchko, G.W., Zhang, Y., Shao, Y., Aksay, I.A., Liu, J., Lin, Y.: Constraint of DNA on functionalized graphene improves its biostability and specificity. Small 6, 1205–1209 (2010)

[11] Novoselov KS, Jiang D, Schedin F, Booth TJ, Khotkevich VV, Morozov SV, Geim AK (2005) Two-dimensional atomic crystals. Proc Natl Acad Sci USA 102(30):10451–10453. doi:10.1073/pnas.0502848102.

[12] Qiu Y, Qu X, Dong J, Ai S, Han R (2011) Electrochemical detection of DNA damage induced by acrylamide and its metabolite at the graphene-ionic liquid-Nafion modified pyrolytic graphite electrode. J Hazard Mater 190(1–3):480–485. doi:10.1016/j.jhazmat.2011.03.071

[13] Bertini I, Lee YM, Luchinat C, Piccioli M, Poggi L (2001) Locating the metal ion in calcium-binding proteins by using cerium(III) as a probe. ChemBioChem 2(7–8):550–558. doi:10.1002/1439-7633(20010803)2:7/8<550:aid-cbic550>3.3.co;2-k

[14] 14.Ohno Y, Maehashi K, Yamashiro Y, Matsumoto K (2009) Electrolyte-gated graphene field-effect transistors for detecting pH protein adsorption. Nano Lett 9(9):3318–3322. doi:10.1021/nl901596m

[15] Lin L, Liu Y, Tang L, Li J (2011) Electrochemical DNA sensor by the assembly of graphene and DNA-conjugated gold nanoparticles with silver enhancement strategy. Analyst 136(22):4732–4737. doi:10.1039/c1an15610a

[16] Liao K-H, Lin Y-S, Macosko CW, Haynes CL (2011) Cytotoxicity of graphene oxide and graphene in human erythrocytes and skin fibroblasts. Acs Appl Mater Interfaces 3(7):2607–2615. doi:10.1021/am200428v

[17] Baby TT, Aravind SSJ, Arockiadoss T, Rakhi RB, Ramaprabhu S (2010) Metal decorated graphene nanosheets as immobilization matrix for amperometric glucose biosensor. Sens Actuators BChem145(1):71–77. doi:10.1016/j.snb.2009.11.022

[18] Fischbein MD, Drndić M. Electron beam nanosculpting of suspended graphene sheets, Applied Physics Letters 2008; 93:113107

[19] S. Garaj, W. Hubbard, A. Reina, J. Kong, D. Branton and J. A. Golovchenko, Nature, 2010, 467, 190-U173.

[20] C. A. Merchant, K. Healy, M. Wanunu, V. Ray, N. Peterman, J. Bartel, M. D. Fischbein, K. Venta, Z. T. Luo, A. T. C. Johnson and M. Drndic, Nano Letters, 2010, 10, 2915-2921.

[21] G. F. Schneider, S. W. Kowalczyk, V. E. Calado, G. Pandraud, H. W. Zandbergen, L. M. K. Vandersypen and C. Dekker, Nano Lett, 2010, 10, 3163-3167.

[22] W. L. Jorgensen, J. Chandrasekhar, J. D. Madura, R. W. Impey and M. L. Klein, J, Chem Phys, 1983, 79, 926-935.

[23] R. M. M. Smeets, U. F. Keyser, D. Krapf, M. Y. Wu, N. H. Dekker and C. Dekker, Nano Letters, 2006, 6, 89-95.

[24] A. D. MacKerell, D. Bashford, M. Bellott, R. L. Dunbrack, J. D. Evanseck, M. J. Field, S. Fischer, J. Gao, H. Guo, S. Ha, D. Joseph-McCarthy, L. Kuchnir, K. Kuczera, F. T. K. Lau, C. Mattos, S. Michnick, T. Ngo, D. T. Nguyen, B. Prodhom, W. E. Reiher, B. Roux, M. Schlenkrich, J. C. Smith, R. Stote, J. Straub, M. Watanabe,

[25] J. Wiorkiewicz-Kuczera, D. Yin and M. Karplus, J Phys Chem B, 1998, 102, 3586- 3616.

[26] L. J. Liang, Q. Wang, T. Wu, T. Y. Sun and Y. Kang, ChemPhysChem, 2013, 14, 2902-2909.

[27] Y. Kang, Z. Zhang, H. Shi, J. Zhang, L. Liang, Q. Wang, H. Ågren and Y. Tu, Nanoscale, 2014, 6, 10666-10672.

[28] B. Hess, C. Kutzner, D. van der Spoel and E. Lindahl, J Chem Theory Comput, 2008, 4, 435-447.

[29] L. Liang, P. Cui, Q. Wang, T. Wu, H. Agren and Y. Tu, RSC Advances, 2013, 3, 2445-2453.

[30] E. A. Manrao, I. M. Derrington, A. H. Laszlo, K. W. Langford, M. K. Hopper, N. Gillgren, M. Pavlenok, M. Niederweis and J. H. Gundlach, Nature Biotechnology, 2012, 30, 349-353.

[31] C. Sathe, X. Q. Zou, J. P. Leburton and K. Schulten, Acs Nano, 2011, 5, 8842-8851.

[32] J. L. Li, D. Stein, C. Qun, E. Brandin, A. Huang, H. Wang, D. Branton and J. Golovchenko, Biophys J, 2003, 84, 134a-135a.

[33] K. S. Novoselov, A. K. Geim, S. V. Morozov, D. Jiang, Y. Zhang, S. V. Dubonos, I. V. Grigorieva, A. A. Firsov, Science 2004, 306, 666.

[34] D. Li, R. B. Kaner, Science 2008, 320, 1170.
[35] D. Li, M. B. Muller, S. Gilje, R. B. Kaner, G. G. Wallace, Nat. Nanotechnol. 2008, 3, 101.
[36] S. Stankovich, D. A. Dikin, G. H. B. Dommett, K. M. Kohlhaas, E. J. Zimney, E. A. Stach, R. D. Piner, S. T. Nguyen, R. S. Ruoff, Nature 2006, 442, 282.
[37] D. D. Dikin, S. Stankovich, E. J. Zimney, R. D. Piner, G. H. B. Dommett, G. Evmenenko, S. T. Nguyen, R. S. Ruoff, Nature 2007, 448, 457.
[38] X. Sun, Z. Liu, K. Welsher, J. T. Robinson, A. Goodwin, S. Zaric, Nano Res. 2008, 1, 203.
[39] N. Mohanty, V. Berry, Nano Lett. 2008, 8, 4469.
[40] R. S. Swathi, K. L. Sebastian, J. Chem. Phys. 2008, 129, 054703.
[41] R. S. Swathi, K. L. Sebastian, J. Chem. Phys. 2009, 130, 086101.
[42] C. Lu, H. Yang, C. Zhu, X. Chen, G. Chen, Angew. Chem. Int. Ed. 2009, 48, 4785.
[43] JM Rothberg et al., Nature, 2011, 475, 348-52.
[44] IY Sohn; DJ Kim; JH Jung; OJ Yoon; TN Thanh; TT Quang; NE Lee, Biosensors and Bioelectronics, 2013, 45, 70–76.
[45] CJ Shih; S Lin; R Sharma; MS Strano; D Blankschtein, Langmuir, 2012, 28, 235–241.
[46] H Wu; W Lu; JJ Shao; C Zhang; M Wu; B Li; Q Yang, New Carbon Mat., 2013, 5(28), 327-335.
[47] S Pei; HM Cheng, Carbon, 2012, 9(50), 3210-3228.
[48] VH Pham; HD Pham; TT Dang; SH Hur; EJ Kim; BS Kong; S Kim; JS Chung, J. Mater. Chem., 2012, 22, 10530-10536.
[49] Akca, S., Foroughi, A., Frochtzwajg, D., Postma, H.W. Competing interactions in DNA assembly on graphene. PLoS ONE 6, e18442 (2011).
[50] Lu, C.H., Yang, H.H., Zhu, C.L., Chen, X., Chen, G.N.: A graphene platform for sensing biomolecules. Angew. Chem. Int. Ed. 48, 4785–4787 (2009)
[51] Li, F., Huang, Y., Yang, Q., Zhong, Z., Li, D., Wang, L., Song, S., Fan, C.: A grapheneenhanced molecular beacon for homogeneous DNA detection. Nanoscale 2, 1021–1026 (2010)
[52] Lu, C.H., Li, J., Liu, J.J., Yang, H.H., Chen, X., Chen, G.N.: Increasing the sensitivity and single-base mismatch selectivity of the molecular beacon using graphene oxide as the "nanoquencher". Chem.-Eur. J. 16, 4889–4894 (2010).
[53] He, S., Song, B., Li, D., Zhu, C., Qi, W., Wen, Y., Wang, L., Song, S., Fang, H., Fan, C.: A graphene nanoprobe for rapid, sensitive, and multicolor fluorescent DNA analysis. Adv. Funct. Mater. 20, 453–459 (2010)
[54] Wu, C., Zhou, Y., Miao, X., Ling, L.: A novel fluorescent biosensor for sequence-specific recognition of double-stranded DNA with the platform of graphene oxide. Analyst 136, 2106–2110 (2011).
[55] Hong, B.J., Compton, O.C., An, Z., Eryazici, I., Nguyen, S.T.: Successful stabilization of graphene oxide in electrolyte solutions enhancement of biofunctionalization and cellular uptake. ACS Nano 6, 63–73 (2012).
[56] Hong, B.J., An, Z., Compton, O.C., Nguyen, S.T.: Tunable biomolecular interaction and fluorescence quenching ability of graphene oxide: application to "turn-on" DNA sensing in biological media. Small 8, 2469–2476 (2012).
[57] Postma, H. W. C. Nano Lett. 2010, 10, 420.
[58] He, Y.; Scheicher, R. H.; Grigoriev, A.; Ahuja, R.; Long, S.; Huo, Z.; Liu, M. Adv. Funct. Mater. 2011, 21, 2674.
[59] Nelson, T.; Zhang, B.; Prezhdo, O. V. Nano Lett. 2010, 10, 3237.
[60] Zwolak, M.; Di Ventra, M. Rev. Mod. Phys. 2008, 80, 141−165.
[61] Tsutsui, M.; Taniguchi, M.; Yokota, K.; Kawai, T. Nat. Nanotechnol. 2010, 5, 286.
[62] Huang, S.; He, J.; Chang, S.; Zhang, P.; Liang, F.; Li, S.; Tuchband, M.; Fuhrmann, A.; Ros, R.; Lindsay, S. Nature Nanotechnol. 2010, 5, 868−873
[63] Zârbo, L. P.; Nikolic′, B. K. Europhys. Lett. 2007, 80, 47001.
[64] Tao, C.; Jiao, L.; Yazyev, O. V.; Chen, Y.-C.; Feng, J.; Zhang, X.; Capaz, R. B.; Zettl, J. M. T. A.; Louie, S. G.; Dai, H.; Crommie, M. F. Nat. Phys. 2011, 7, 616.
[65] Hasan, M. Z.; Kane, C. L. Rev. Mod. Phys. 2010, 82, 3045−3067.
[66] Areshkin, D.; White, C. Nano Lett. 2007, 7, 3253−3259.
[67] Weeks, C.; Hu, J.; Alicea, J.; Franz, M.; Wu, R. Phys. Rev. X 2011, 1, 021001.
[68] Cai, J.; Ruffieux, P.; Jaafar, R.; Bieri, M.; Braun, T.; Blankenburg, S.; Muoth, M.; Seitsonen, A. P.; Saleh, M.; Feng, X.; Mullen, K.; Fasel, R. Nature 2010, 466, 470−473.
[69] Jia, X.; Hofmann, M.; Meunier, V.; Sumpter, B. G.; Campos- Delgado, J.; Manuel, J.; Hyungbin, R.-H.; Ya-Ping, S.; Reina, H. A.; Kong, J.; Terrones, M.; Dresselhaus, M. S. Science 2009, 323, 1701.
[70] Meunier, V.Krstić, P. S. J. Chem. Phys. 2008, 128, 041103.
[71] Prasongkit, J. Grigoriev, A.; Pathak, B.; Ahuja, R.; Scheicher, R. H. Nano Lett. 2011, 11, 1941−1945.
[72] Sorgenfrei, S. et al. Label-free single-molecule detection of DNA-hybridization kinetics with a carbon nanotube field-effect transistor. Nat. Nanotech. 6, 126– 132 (2011).
[73] Hahm, J. & Lieber, C. M. Direct ultrasensitive electrical detection of DNA and DNA sequence variations using nanowire nanosensors. Nano Lett. 4, 51–54 (2004)
[74] MAQC Consortium. The MicroArray Quality Control (MAQC) project shows inter- and intraplatform reproducibility of gene expression measurements. Nat. Biotechnol. 24, 1151–1161 (2006).
[75] Dalma-Weiszhausz, D. D.Warrington, J., Tanimoto, E. Y. & Miyada, C. G. The Affymetrix GeneChips platform: an overview. Methods Enzymol. 410, 3–28 (2006).
[76] Chen, T. et al. Label-free detection of DNA hybridization using transistors based on CVD grown graphene. Biosens. Bioelectron. 41, 103–109 (2013).
[77] Cai, B. et al. Ultrasensitive label-free detection of PNA-DNA hybridization by reduced graphene oxide field-effect transistor biosensor. ACS Nano 8, 2632–2638 (2014).

[78] The Affy Metrix DNA Microarray website (http://www.affymetrix.com/ Accessed 15 June 2014).
[79] Yao, X. et al. Sub-attomole oligonucleotide and p53 cDNA determinations via a high-resolution surface plasmon resonance combined with oligonucleotidecapped gold nanoparticle signal amplification. Anal. Biochem. 354, 220–228 (2006).
[80] Taton, T. A., Mirkin, C. A. & Letsinger, R. L. Scanometric DNA array detection with nanoparticle probes. Science 289, 1757–1760 (2000).
[81] Song, L., Ahn, S. & Walt, D. R. Fiber-optic microsphere-based arrays for multiplexed biological warfare agent detection. Anal. Chem. 78, 1023–1033 (2006).
[82] Bowden, M., Song, L. & Walt, D. R. Development of a microfluidic platform with an optical imaging microarray capable of attomolar target DNA detection. Anal. Chem. 77, 5583–5588 (2005).
[83] Gao, Z. Q., Rafea, S. & Lim, L. H. Detection of nucleic acids using enzymecatalyzed template-guided deposition of polyaniline. Adv. Mater. 19, 602–606 (2007).
[84] Azek, F., Grossiord, C., Joannes, M., Limoges, B. & Brossier, P. Hybridization assay at a disposable electrochemical biosensor for the attomole detection of amplified human cytomegalovirus DNA. Anal. Biochem. 284, 107–113 (2000).
[85] Takenaka, S., Yamashita, K., Takagi, M., Uto, Y. & Kondo, H. DNA sensing on a DNA probe-modified electrode using ferrocenylnaphthalene diimide as the electrochemically active ligand. Anal. Chem. 72, 1334–1341 (2000).
[86] Xie, H., Zhang, C. & Gao, Z. Amperometric detection of nucleic acid at femtomolar levels with a nucleic acid/electrochemical activator bilayer on gold electrode. Anal. Chem. 76, 1611–1617 (2004).
[87] Ghindilis, A. L. et al. CombiMatrix oligonucleotide arrays: genotyping and gene expression assays employing electrochemical detection. Biosens. Bioelectron. 22, 1853–1860 (2007).
[88] Gurtner, C. et al. Microelectronic array devices and techniques for electric field enhanced DNA hybridization in low-conductance buffers. Electrophoresis 23, 1543–1550 (2002).
[89] Wang J. Cai, X. Wang J. Jonsson, C. & Palecek, E. Trace measurements of RNA by potentiometric stripping analysis at carbon paste electrodes. Anal. Chem. 67, 4065–4070 (1995).
[90] Wang J. Zhang X. Parrado, C. & Rivas, G. Controlled release of DNA from carbon-paste microelectrodes. Electrochem. Commun. 1, 197–202 (1999).
[91] Li, X. et al. Transfer of large-area graphene films for high-performance transparent conductive electrodes. Nano Lett. 9, 4359–4363 (2009).
[92] Reina, A. et al. Large area, few-layer graphene films on arbitrary substrates by chemical capor deposition. Nano Lett. 9, 30–35 (2009).
[93] Cohen-Karni, T. Qing, Q. Li, Q. Fang, Y. & Lieber, C. M. Graphene and nanowire transistors for cellular interfaces and electrical recording. Nano Lett. 10, 1098–1102 (2010).
[94] Hess, L. H. et al. Graphene transistor arrays for recording action potentials from electrogenic cells. Adv. Mater. 23, 5045–5049 (2011).
[95] Z.W. Tang, , H. Wu, J.R. Cort, G.W. Buchko, Y. Zhang, Y. Shao, I.A. Aksay, J. Liu, Y. Lin. Constraint of DNA on functionalized grapheme improves its biostability and specificity. Small. 6: 1205, 2010.
[96] Y. Lu, J.W. Liu. Functional DNA nanotechnology: emerging applications of DNAzymes and aptamers. Curr. Opin. Biotechnol. 17: 580, 2006.
[97] C.H. Lu, H.H. Yang, C. L. Zhu, X. Chen, G.N. Chen. A graphene platform for sensing biomolecules. Angew. Chem. Int. Ed. 48: 4785, 2009.
[98] H. Jang, Y. K. Kim, H. M. Kwon, W. S. Yeo, D. E. Kim, D. H. Min. A graphene-based platform for the assay by helicase. Angew. Chem. Int. Ed. 49: 5703, 2010.
[99] S.J. He, B. Song, D. Li, C. Zhu, W. Qi, Y. Wen, L. Wang, S. Song, H. Fang and C. Fan. A graphene nanoprobe for rapid, sensitive, and multicolor fluorescent DNA analysis. Adv. Funct. Mater. 20: 453, 2010.
[100] C.H. Lu, J. Li, J.J. Liu, H.H. Yang, X. Chen, G.N. Chen. Increasing the sensitivity and single-base mismatch selectivity of the molecular beacon using graphene oxide as the nanoquencher. Chem. Eur. J. 16: 4889, 2010.
[101] Y.Q. Wen, F. Xing, S. He, S. Song, L. Wang, Y. Long, D. Li, C. Fan. A graphene-based fluorescent nanoprobe for silver (I) ions detection by using graphene oxide and a silver-specific oligonucleotide. Chem. Commun. 46: 2596, 2010.
[102] H.X. Chang, et al. Graphene fluorescence resonance energy transfer aptasensor for the thrombin detection. Anal. Chem. 82: 2341, 2010.
[103] C.H. Lu, C.L. Zhu, J. Li, J.J. Liu, X. Chen, H.H. Yang. Using graphene to protect DNA from cleavage during cellular delivery. Chem. Commun. 46: 3116, 2010.
[104] F. Liu, J. Y. Choi, T. S. Seo. Graphene oxide arrays for detecting specific DNA hybridization by fluorescence resonance energy transfer. Biosens. Bioelectron. 25: 2361, 2010.
[105] P.R. Selvin. The renaissance of fluorescence resonance energy transfer. Nat. Struct. Biol. 7: 730, 2000.
[106] D.Chen, L. Tang, J. Li. Graphene-based materials in electrochemistry. Chem. Soc. Rev. 39: 3157, 2010.